IEEE Access
Multidisciplinary ⋮ Rapid Review ⋮ Open Access Journal

Received 20 September 2023, accepted 6 October 2023, date of publication 16 October 2023, date of current version 23 October 2023.

Digital Object Identifier 10.1109/ACCESS.2023.3324816

RESEARCH ARTICLE

Wearable UHF-RFID Sensor for Wetness Detection

MELTEM TEKCIN[1], MERIH PALANDOKEN[2], (Senior Member, IEEE), AND SENEM KURSUN[3,4]

[1]Textile Engineering Department, İstanbul Technical University, 34437 İstanbul, Turkey
[2]Electrical and Electronics Engineering Department, İzmir Katip Celebi University, 35620 İzmir, Turkey
[3]Mechanical Engineering Department, İstanbul Technical University, 34437 İstanbul, Turkey
[4]Center of Excellence for Textiles (CETEX), 34467 Istanbul, Turkey

Corresponding authors: Meltem Tekcin (tekcin@itu.edu.tr) and Senem Kursun (kursuns@itu.edu.tr)

This work was supported by the Scientific, and Technological Research Council of Turkey (TUBITAK) under Project 119M976.

ABSTRACT The use of wearable textile Radio Frequency Identification (RFID) sensors is becoming widespread in many different application areas because of their technical utilization advantages. In this study, a textile-based Ultra High Frequency (UHF) RFID sensor that can be used to detect wetness has been developed and fabricated with a pad printing machine using silver conductive ink. The overall physical dimension of the proposed sensor structure is 75.0 mm × 38.0 mm × 0.12 mm. Two different types of Received Signal Strength Indicator (RSSI) measurement setups in near field region and at practical separation distances emulating more realistic environmental conditions have been carried out to test and validate the applicability of the proposed sensor. Water, saline and urine solutions have been used to evaluate different wetting conditions in the near field RSSI measurements by dropping different solutions on the RFID sensor integrated diaper. A permissible signal difference of at least 17 dBm has been detected between the wet and dry states of the proposed wetness detection sensor. The performance of the proposed RFID sensor has been evaluated using different separation distances of 32 cm, 40 cm and 50 cm with the practical result of maximum reading range to be 50 cm for the reliable determination of the binary wetness states. In addition, the performance of the RFID wetness sensor against different bending and deformation conditions is almost robust. It is concluded that the proposed sensor structure can be integrated onto the patient's diapers to facilitate the reliable detection of wetness states in cases such as urinary incontinence in remote health monitoring systems.

INDEX TERMS Diaper, printing, received signal strength indicator (RSSI), RFID sensor, textile based-sensor, ultra high frequency (UHF), urinary incontinence, wearable, wetness detection.

I. INTRODUCTION

Radio Frequency Identification (RFID) is defined as a low-cost wireless technology that is used in businesses to identify products, locate, and communicate, as well as establish connections between numerous objects [1]. The use of RFID technology in many different application areas is becoming widespread. Health monitoring [2], [3], goods [4] or patient tracking systems [5], and logistics [6], [7] are the areas where RFID technology is frequently used. The design and operating frequency of RFID sensors are determined according to the needs of their usage areas, and sensing functions [8]. Generally, there are three different frequency bands used for RFID tags. These frequency bands are the low frequency band (120–150 kHz), the high frequency band (13.56 MHz), and the ultra-high frequency band (433 MHz, 865–868 MHz in Europe, 917–922 MHz in China and 902–928 MHz in North America) [9], [10]. Recently, Ultra High Frequency (UHF) RFID tags and sensors are highly preferred due to several advantages. Among these advantages are the low cost, long-distance operation, and fast-easy identification of UHF-RFID devices [8], [11].

Textile UHF RFID sensors have emerged as a result of the combination of sensing data wirelessly with flexible, and

The associate editor coordinating the review of this manuscript and approving it for publication was Parikshit Sahatiya.

wearable substrates. The signal strength indicator parameter is a typical method used to detect data wirelessly [8], [12], [13]. Received Signal Strength Indicator (RSSI) is an important parameter which shows the signal strength received from RFID tag to RFID reader in RFID systems for communication to take place. There are limits that the reader, and chip used in the RFID system, and these limits show the sensitivity of the reader, and the chip. For communication to take place, the RSSI value must be within these limits. Although RSSI value changes depending on antenna gain, distance between antenna, and path loss, RFID tag can be designed to function as a sensor according to RSSI value, since it can also be affected by different conditions. In this study, it is aimed to design textile-based RFID structure to act as a sensor according to the received signal against different wetness levels.

Wetness detection systems for individuals are generally developed for sweat, blood, skin wetness sensing and urinary incontinence situations. In this study, urinary incontinence was chosen for wetness detection. Urinary incontinence is the involuntary leakage of urea during exertion and in situations such as coughing and sneezing [14]. Urinary incontinence can affect many conditions such as social, psychological, physical and family life of the patient, and this situation reduces the life quality of people and limits their social lives [15], [16]. Although there are many treatments for urinary incontinence, none of these treatments are completely curative [17]. For this reason, urinary incontinence patients have to use diapers. Diaper changes of urinary incontinence patients in hospitals and nursing homes are done by caregivers and health personnel. Caregivers check these individuals very often, as wet diapers on patients and the elderly cause various diseases such as dermatitis and infection [18], [19]. While these controls are an extra workload for the caregiver, they also cause the patients to be awakened and disturbed [18]. For these reasons, there is a need wetness detection system that detect when diaper changes are necessary.

Textile-based UHF-RFID sensors are lightweight, washable, flexible, and wearable compared to conventional UHF-RFID sensors. This situation ensures the use of textile-based RFID sensors to increase day by day [9]. In a study, a wearable knitted UHF-RFID compression sensor antenna has been proposed for respiratory monitoring. As a result of the tests performed on the reusable UHF-RFID sensor, the radiation efficiency on the body has shown good values with permissible sensitivity to the compression [12]. In another study, textile-based UHF-RFID antennas produced by embroidery method have been applied to surgical masks. The maximum reading distance of the UHF-RFID antenna placed on the surgical mask has been measured as 1.1 meters. It has been emphasized that the proposed design can provide identification or safe distance warning in case of an epidemic [20]. In another study using the embroidery method, the moisture sensing performance of the textile-based UHF-RFID antenna has been investigated. As a result, it has been shown that the use of RFID technology in moisture sensing studies is very advantageous [21]. UHF-RFID antenna performance has been investigated by applying different heat treatments to the wearable sensor produced using the printing method. According to the results obtained, it is stated that the proposed sensor structure can be used as a UHF-RFID antenna, especially in areas sensitive to humidity [22]. In the study of Sen et al., moisture detection has been made with UHF RFID moisture monitoring by utilizing absorbent polymers in diapers. The proposed sensor structure has been designed using metal and hydrogel in accordance with the diaper geometry [23]. Bluetooth-based detector developed for babies and the elderly detects wetness and bleeding. The wetness sensor consisting of two or four conductive thin wires has been connected to pressing studs which placed in the diaper or bandage. When the wires inside the diaper or bandage come into contact with blood or urine, the conductivity of the pressing studs exceeds the predetermined threshold value, informing its wetness status [24]. A sensor mat that can be placed under the sheets was recommended to detect urinary incontinence and bed occupancy. This sensor consists of embroidered conductive yarns. While the wetness is detected by looking at the resistance change of the sensor, the occupancy status was determined by the capacitance change. An external unit consisting of radio frequency (RF) connection or WiFi module has been used for recording and transferring the obtained data [25].

There are many printing methods available today and it is extremely important to select the appropriate printing method for printed electronic structures to perform at their best. Printing technologies consist of two main groups; contact, and non-contact methods. In contact printing method, the surface with ink is in direct contact with the substrate, while in non-contact printing method, the ink prepared in solution is dispersed or sprayed onto the substrate [26]. Inkjet [27], [28], and aerosol jet printing [29] techniques are the examples of non-contact printing methods. On the other hand, some kinds of contact printing techniques are screen printing [30], gravure printing [31], flexographic [32], and pad printing [22] methods. Pad printing, which is a versatile offset printing technique, is one of the oldest printing techniques. Thanks to the developments in pad printing, the application areas of pad printing have expanded from conventional textiles to sensors, biosensors, RFID tags, and photovoltaic cells [33], [34]. The first step in the pad printing method is to create the desired pattern on the printing plate called cliché. Then, the ink reservoir comes over this pattern and the ink covers the pattern. At this point, the important thing is to remove the excess ink from the cliché very well. Finally, the silicone pad first takes the pattern onto itself and then transfers it to the substrate [22], [34], [35]. Pad printing becomes advantageous when compared to other printing methods due to its low cost, simplicity, fastness, ability to work even with high

viscosity inks, printing on a wide variety of substrates like flexible, curved, and rough surfaces, and printing layer by layer [33].

Literature reveals that many textile-based sensors and antennas have been introduced. However, the difference of the current study compared to the alternative sensor designs in the literature is that it proposes a novel sensor design that senses through the RSSI level for the wetness detection. Thus, in this study, textile-based wearable and flexible UHF-RFID sensor is designed, numerically computed, and printed on polyamide-based taffeta label fabric according to the pad printing method using silver conductive ink. After RFID chip is integrated onto the printed RFID sensor, water, saline and urine solution have been dropped onto the fabricated RFID sensor for wetness detection measurements. Wetness performance of the produced RFID sensor structure is determined by detecting the RSSI changes in the RFID sensor with the help of RFID reader antenna. RFID sensor structure used in the study can also be integrated onto baby diapers to detect urinary incontinence in babies. However, the study targets urinary incontinence in adults, as diaper changes are easier in infants than in elderly and sick adults. The presented study is one of the rare studies that uses the RSSI sensing principle to detect urinary incontinence through the pad printed RFID sensor geometric model with the chip integration. The novelty of the study is that the disposable, flexible, textile-based RFID sensor to be designed and fabricated for this application can be produced by a very simple printing method, and it is very thin and small to provide users' comfort with the biocompatible feature.

II. MATERIALS AND METHODS

A. CHEMICALS, MATERIALS AND INK FORMULATION

In this study, silver conductive ink has been used to produce e-textile based UHF-RFID wetness sensor. To adapt the viscosity of silver conductive ink having 10.000 cP dynamic viscosity to the pad printing method, a thinner from TRI Electronic is used. Polyamide-based taffeta label fabric supplied by Huzhou Hengxin Label Manufacture Co. (Huzhou, China) is used as a substrate for printing the UHF-RFID wetness sensor. The technical characteristics of the substrate have been detailed in the previous study [28]. Impinj Monza R6-P tag chip was purchased to connect the UHF-RFID wetness sensor with the RFID reader. The optimum ink formulation for pad printing is given in [22].

B. UHF-RFID WETNESS SENSOR DESIGN, SIMULATION AND FABRICATION

While RFID sensor circuit performance is greatly influenced by the frequency-dependent complex impedance of the chip to be integrated after the fabrication of the sensor model, the input impedance of whole sensor geometric model has to be determined through the parametric analysis and optimizations. Therefore, the input impedance of the chip is firstly obtained from the datasheet after the RFID chip to be integrated has been determined. In this study, Impinj Monza R6-P RFID chip is selected. The complex chip impedance at 867 MHz is nearly equal to 18.27 - j146.7 Ω, which is additionally checked through the fabricated directional coupler. After the chip impedance is obtained, the impedance of RFID sensor structure is designed to be complex conjugated with the impedance of the chip to be integrated. The RFID sensor model is shown in Figure 1 along with the geometric parameters in Table 1. The proposed sensor model is composed of E-shaped resonator and modified U-shaped resonator loaded with the T-shaped extended stub where the RFID chip is to be connected in between. The structural model of the proposed sensor has been designed and numerically calculated in Microwave CST Studio. The discrete port impedance has been set to 18.27 Ω and the required amount of capacitance representing the reactive part of RFID chip has been modelled through the capacitance lumped element of 1.25 pF in the numerical model as shown in Figure 1. Therefore, the discrete port representing the RFID chip has been completely modelled through the series combination of discrete capacitance and port resistance with the respective values of 1.25 pF and 18.27 Ω. The substrate material has been selected as polyamide based taffeta with the relative permittivity and loss tangent of 2 and 0.02, respectively. The metal parts have been selected as silver. The overall dimensions of the proposed sensor structure are 75.0 mm × 38.0 mm × 0.12 mm.

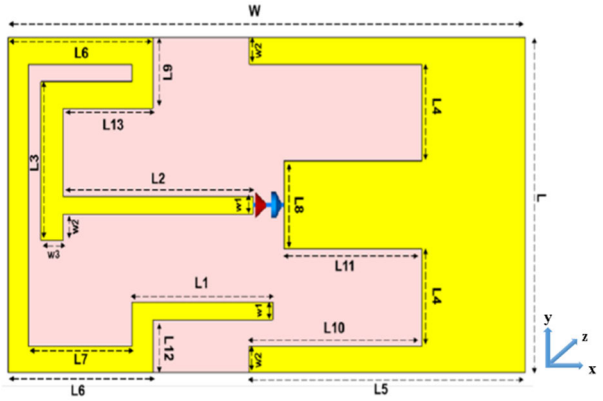

FIGURE 1. Proposed RFID sensor structure.

TABLE 1. Dimensions of proposed RFID sensor structure.

Symbol	Size	Symbol	Size
L	75 mm	**L5**	40 mm
W	38 mm	**L6**	21 mm
W1	2 mm	**L7**	15 mm
W2	3 mm	**L8**	10 mm
W3	3.25 mm	**L9**	8 mm
L1	20.40 mm	**L10**	25 mm
L2	27.50 mm	**L11**	20 mm
L3	18 mm	**L12**	6 mm
L4	11 mm	**L13**	13 mm

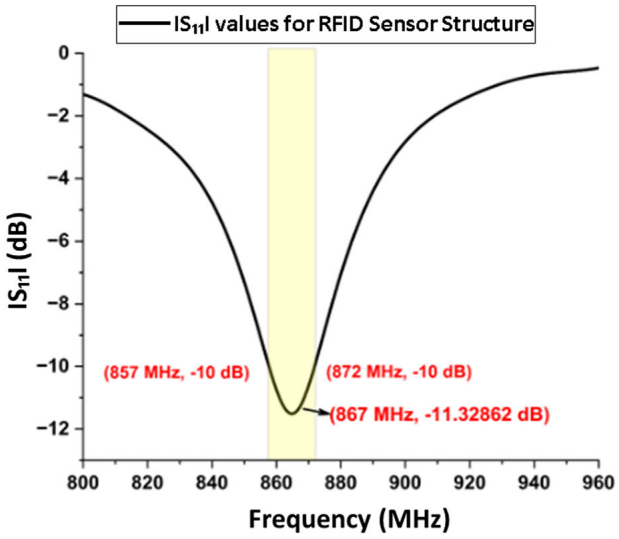

FIGURE 2. |S11| parameter of RFID sensor structure at 867 MHz.

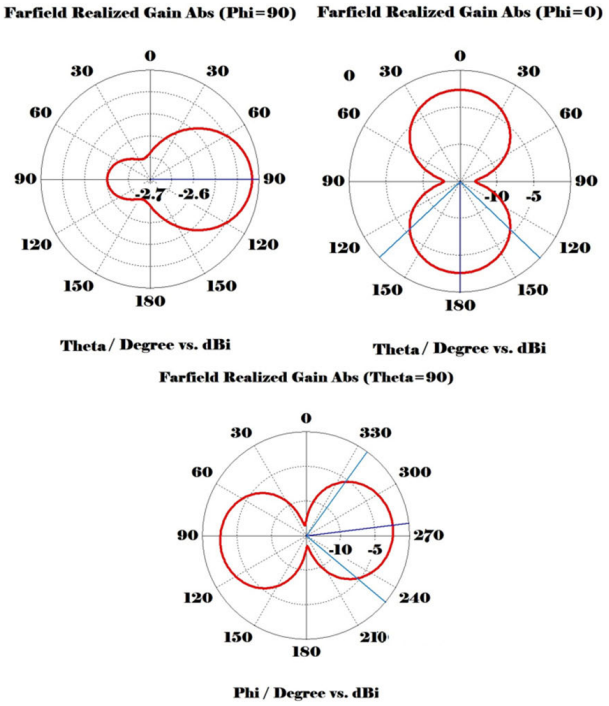

FIGURE 3. 2D polar radiation patterns for RFID sensor structure.

The input reflection parameter of the proposed RFID wetness sensor integrated with the RFID chip is shown in Figure 2 to point out the impedance matching between the sensor geometric model and the RFID chip. As deduced from Figure 2, the RFID sensor structure operates in the frequency band of 857 MHz and 872 MHz with the resonance frequency of 867 MHz. The polar radiation patterns for X-Y, X-Z, and Y-Z planes, and surface current distribution of RFID sensor structure at 867 MHz have been shown in Figure 3 and Figure 4, respectively.

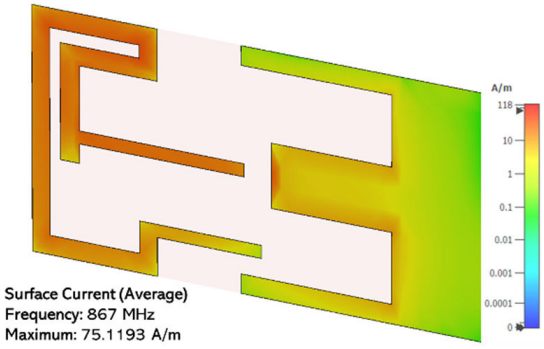

FIGURE 4. Surface current distribution at 867 MHz.

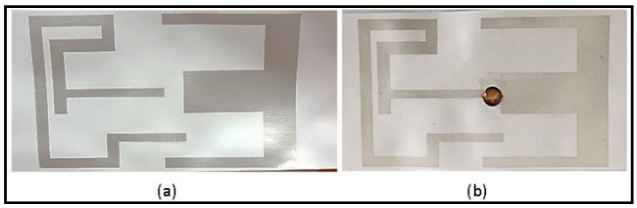

FIGURE 5. a) Printed RFID sensor structure (b) Printed RFID sensor structure with chip integration.

The surface current distribution in Figure 4 shows which sensor sections in the main resonator geometry are more prone to the liquid drops to obtain possibly high value of RSSI value changes between the dry and wet states of RFID wetness sensor. This provides additional practical information on how the relative placement of RFID wetness sensor has to be managed in the adult diaper with the targeted consequence of increased exposure level of wetness sensor to more liquid drops.

After the RFID wetness sensor model has been verified through the numerical computations, the fabrication of the sensor has been carried out. To fabricate the RFID sensor structure, according to determined dimensions based on the simulation results, a pad printing method is used and a cliché is prepared. COMEC, EAZY90 pad printing machine has been used in the study. The working principle of the pad printing machine (COMEC, EAZY90) is explained in [22].

Printing process is carried out using cliché and silver ink for which the prescription is given on the polyamide-based taffeta label fabric. The print pass number has been determined as 3 to increase the conductivity of the RFID sensor. After each print, drying process is applied for 2 minutes in order to avoid print slipping. Finally, the sintering process is applied on the printed RFID sensor in an oven at 150°C for 30 minutes.

After this process, the RFID IC must be connected to the RFID sensor in order to make the sensor ready for the measurement with RFID reader. The RFID IC has two contact pads and it has been mounted on the sensor through these contact pads using conductive paste and ready for the measurement. The printed RFID sensor and the chip integrated to the RFID sensor are shown in Figure 5.

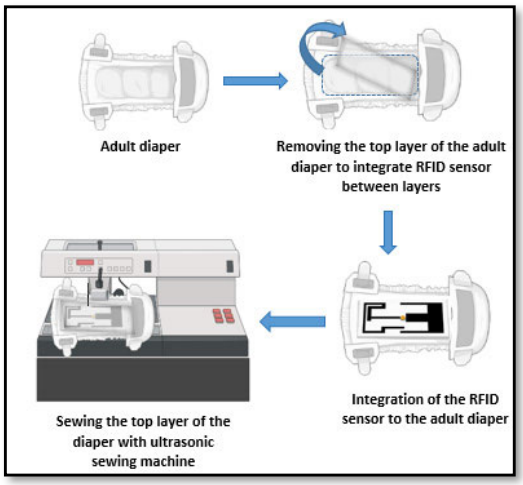

FIGURE 6. Schematic view of the integration of the RFID sensor into the diaper.

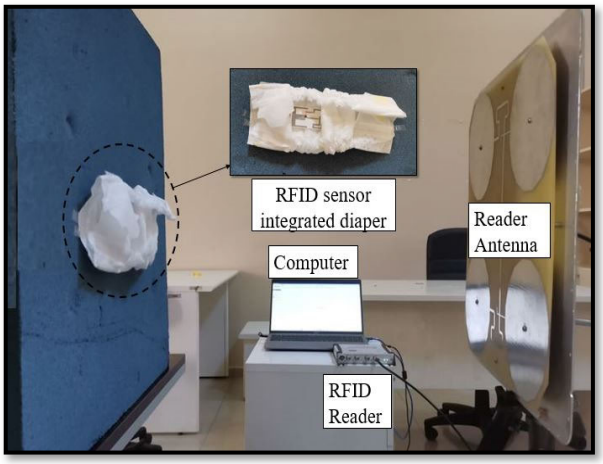

FIGURE 8. RSSI measurement setup with highly directive 2 × 2 antenna array at practical separation distances emulating the real life.

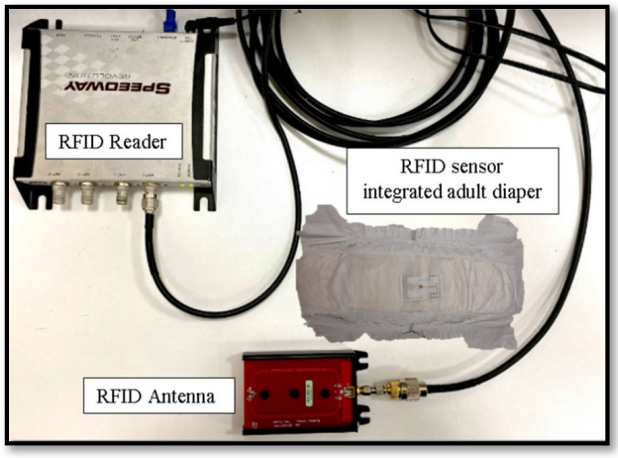

FIGURE 7. RSSI near field measurement setup.

C. INTEGRATION OF THE RFID SENSOR ONTO ADULT DIAPER FOR RSSI MEASUREMENTS

RFID sensor is printed on adhesive polyamide-based taffeta fabric for easy integration of the RFID sensor onto the adult diaper. The adult diaper consists of many different layers. In order for the RFID sensor not to come into direct contact with the skin, the sensor must be placed between the layers. Therefore, the top layer of the diaper is removed and the RFID sensor is placed between the top layer of the diaper and the ADL (Acquisition/Distribution Layer). Then, the top layer separated to restore the original form of the diaper is sewn to the diaper with an ultrasonic sewing machine. The schematic view of the process is shown in Figure 6.

For RSSI measurements, different amounts of water, saline, and urea solutions have been dropped onto the RFID sensor integrated into the adult diaper, and RSSI values are measured with the help of a near field RFID reader through near field communication. Figure 7 indicates the schematic view of the near-field RSSI measurement setup. The near-field RSSI measurements are performed as preliminary test and validation steps in the scope of proof of concept in order to observe whether the detectable amount of changes in RSSI levels could be obtained between the wet and dry states of RFID wetness sensor in near field reading ranges.

Near field RSSI measurement results can be basically affected by the relative positioning of the RFID sensor with respect to reader antenna on which the RFID wetness sensor has been directly located in addition to other nearby substances in the environment and ambient conditions [36], [37]. For these reasons, attention is paid to ensure that the substances in the environment are at the same distance and position in each measurement to preserve the same measurement conditions. However, in order to investigate the wetness detection performance of the RFID wetness sensor at practical reading distances, in addition to the measurement setup indicated in Figure 7, versatile measurements have been carried out by using highly directive antenna array for RFID wetness sensor in salty water at different polarization orientations. The measurement setup shown in Figure 8 has been arranged to emulate the RFID wetness sensor embedded patient diaper-reader antenna distances in the real-life environment.

In real life, it is appropriate to locate the reader antenna at a practical separation distance of 40 cm from the diaper under the patients bed at right antenna orientation. Moreover, in order for the proposed RFID wetness sensor to be used in real life, the RSSI values obtained from the RFID reader have to be firstly calibrated with previously measured data in the wetness detection environment as in other sensor applications. Based on the laboratory measurement results, it can be deduced that the circular polarized antenna can be conveniently used as a reader antenna to increase the RSSI level for the better detection of wetness level in large amounts

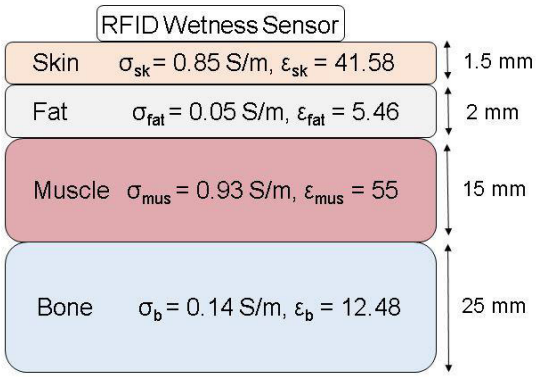

FIGURE 9. Four layered human body phantom model.

of urine in addition to the utilization of new generation RFID systems with lower reading sensitivity levels.

D. BENDING SIMULATION AND BENDING MEASUREMENT OF RFID SENSOR STRUCTURE

In order to make the RFID sensor structure printed on the flexible label fabric wearable, the proposed structure should be resistant to bending, stretching, and other deformations [38]. For this, bending simulations and deformation tests have been applied to the sensor structure. The performance of the RFID sensor against different bending conditions has been simulated in the CST Studio [39]. During the simulations, different bending angles, 15°, 45°, 90°, − 15°, − 45°, and − 90°, were applied to the structure. Apart from the numerical computation, a manual deformation test has been carried out by combining the right and left edges of the RFID sensor integrated adult diaper at the middle point [40]. This process has been done 10 times.

The proposed RFID wetness detection sensor can be subject to different bending states in practical applications when it is placed into the adult diaper, which has been worn on the human body. A human body phantom has been therefore modelled to gain more information about the change in the input impedance of the RFID sensor affecting the measured RSSI values under these bending conditions. Considering four-layered human body model, parametric numerical computations of RFID sensor have been conducted for varying bending angles. The four-layered human body model consists of skin ($\sigma_{sk} = 0.85$ S/m and $\varepsilon_{sk} = 41.58$), fat ($\sigma_{fat} = 0.05$ S/m and $\varepsilon_{fat} = 5.46$), muscle ($\sigma_{mus} = 0.93$ S/m and $\varepsilon_{mus} = 55$) and bone ($\sigma_b = 0.14$ S/m and $\varepsilon_b = 12.48$) [41], [42]. The RFID wetness sensor has been located on the top of all these four layers with the bending angles ranging from 15° up to 90° with 15° steps. The schematic view of four layered human body model is shown in Figure 9.

III. RESULTS AND DISCUSSION

The proposed RFID sensor structure shows the varying sensing performance due to the input impedance change and respective degradation in gain as a result of nearfield coupling to the exposed liquid drops and the corresponding change in RSSI value to be deduced from the Friis Transmission equation shown below:

$$P_R = P_T \frac{G_T\left(\theta_T, \emptyset_T\right) G_R\left(\theta_R, \emptyset_R\right) \lambda^2}{(4\pi r)^2}(1 - |\Gamma_T|^2)(1 - |\Gamma_R|^2) \times \left|\hat{p}_T . \hat{p}_R\right|^2 \quad (1)$$

The term P_R in the equation represents the power received by RFID sensor structure, P_T term is the power transmitted by RFID reader antenna, whereas the G_T indicates RFID reader antenna gain and the G_R represents RFID sensor structure gain and r denotes the distance between the reader antenna and the RFID sensor structure. The term $(1-|\Gamma_T|^2)(1-|\Gamma_R|^2)$ represents the transmission loss due to the reflection, $\left|\hat{p}_T . \hat{p}_R\right|^2$ term indicates the losses due to the polarization mismatch. For a reliable communication to be realized between the RFID reader and the RFID wetness sensor, the reading sensitivity of the whole reader system imposed by the RFID chip used in the sensor structure is extremely important. The RFID reader in the current study can achieve the reading capability up to −84 dBm RSSI level. However, since distance and environmental factors influence the sensing capability of the proposed sensor structure, these parameters have been tried to be kept constant in all near field measurements for different situations.

In the measurement process, RSSI values have been obtained with the measurement software of the RFID reader. To detect the wetness, different amounts of salt water mixture have been dropped onto different points of the sensor structure by using a dropper, and the response of the structure for these different situations has been determined through RSSI measurements. Figure 10 shows the variation of RSSI values according to different salt water amounts in near field measurements. When Figure 10 is examined, the RSSI value of the designed sensor structure is − 35.31 dBm in the dry state, while a certain amount of degradation in RSSI value is then observed when water and saltwater mixtures are dropped in different amounts. Measurements have been made using a reader antenna with a gain of 2 dBi in the near field. When water has been dropped over 100 mL on the sensor structure, it could not be read from RFID reader because the sensitivity of the RFID reader is − 84 dBm. Since all environmental values are kept constant during the measurement, the reason for the RSSI change is that water and saltwater drops affect the gain of the RFID sensor structure.

Especially in health monitoring applications, both the health personnel and the patient have difficulties in determining the urinary incontinence status of adult patients. In order to prevent this situation, an easy-to-fabricate RFID wetness sensor providing remote warning and directly integrable to diaper is needed. In order to test RFID sensor performance with a diaper, different solutions containing saline, and urine have been prepared and poured onto diaper where the RFID

TABLE 2. RSSI levels for different situations on RFID sensor structure.

RFID sensor situation	Average RSSI (dBm)
Dry	- 35.49
12 mL water	- 41.19
Between moist nonwoven surface	- 48.52
Between very wet nonwoven surface	- 52.77
Between salty and moist nonwoven surface	- 49.22
Between salty and very wet nonwoven surface	- 54.35
Between nonwoven surfaces moistened with urine solution	- 42.00
Between nonwoven surfaces wetted with urine solution	- 50.50

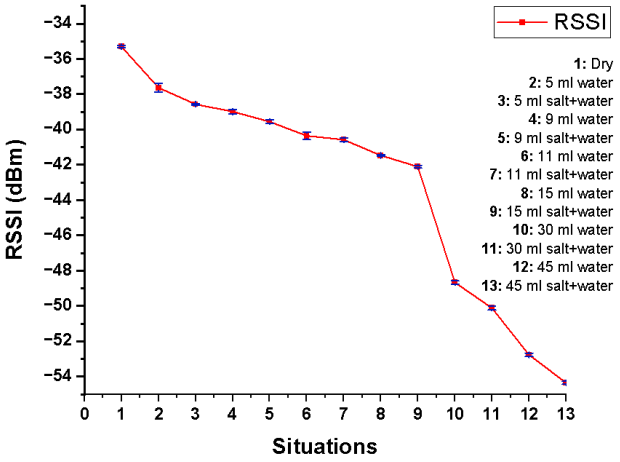

FIGURE 10. RSSI levels for different salt water amounts on RFID sensor structure.

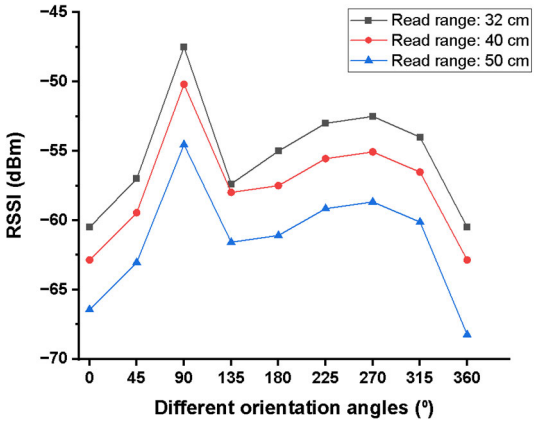

FIGURE 11. RSSI values of RFID sensor structure for different orientation angles with the separation distance of 32 cm, 40 cm, and 50 cm.

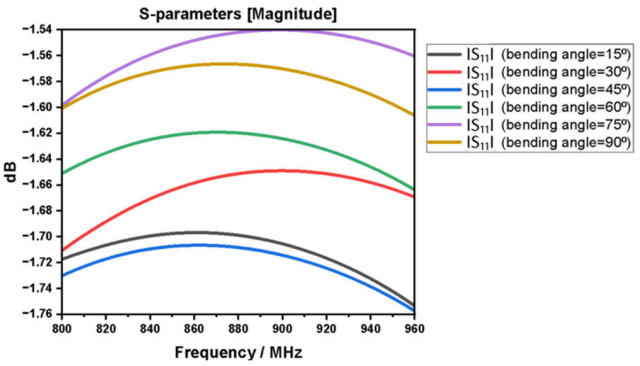

FIGURE 12. |S11| values of RFID sensor structure placed on the human body model against different bending angles.

sensor is hidden between diapers' layers. Urine solution is prepared with 20 mL of distilled water, 0.4 g of urea, and 0.2 g of NaCl. Table 2 shows the RSSI values measured in the sensor structure for different situations.

When Table 2 is examined, it is seen that the RFID sensor structure responds to different wetness conditions in the direction of lower RSSI value as observed in previous measurements. Since the purpose of the sensor is to detect wetness, it is seen that it meets the main purpose of use. The sensor structure is thought to be suitable for detecting the wetness of any textile-based product in different situations.

On the other hand, in more practical situations realized in the measurement setup shown in Figure 8, the maximum RSSI level received by the reader antenna for the RFID sensor immersed in 6 mg / mL salt water from a distance of 50 cm is − 55.24 dBm. Therefore, the maximum reliable reading range of the RFID sensor is considered to be 50 cm. The minimum RSSI level received for the different polarizations is − 68.24 dBm. The maximum and minimum RSSI levels received by the reader antenna are still higher than the sensitivity of the RFID reader module, whose reading sensitivity level is − 84 dBm.

Moreover, the reading ranges have been checked through versatile RSSI measurements while changing orientation angles of RFID sensor with respect to RFID reader antenna set at fixed orientation. RSSI values obtained at different orientation angles for reading ranges of 32 cm, 40 cm and 50 cm have been indicated in the Figure 11. Different orientation angles from 0° to 360° with 45° increments have been selected to change the position of the RFID sensor. These RSSI measurements have been carried out by placing the RFID sensor in 6 mg / mL salt water. According to the Figure 11, RFID sensor gives permissible RSSI results for different orientations at all reading distances between 32 cm and 50 cm to detect the wetness state. Therefore, it has been determined that the different orientation of the RFID sensor with respect to the reader antenna is not a major disadvantage at the reading ranges up to 50 cm. When the effect of different reading distances has been examined at fixed relative orientation of 90° between RFID wetness sensor and reader antenna for maximum RSSI value, the measured RSSI values at the separation distances of 32 cm, 40 cm, and 50 cm are − 47.50 dBm, −50.18 dBm, and − 55.24 dBm, respectively.

|S11| results of the RFID wetness sensor placed on four layered human body model against different bending angles

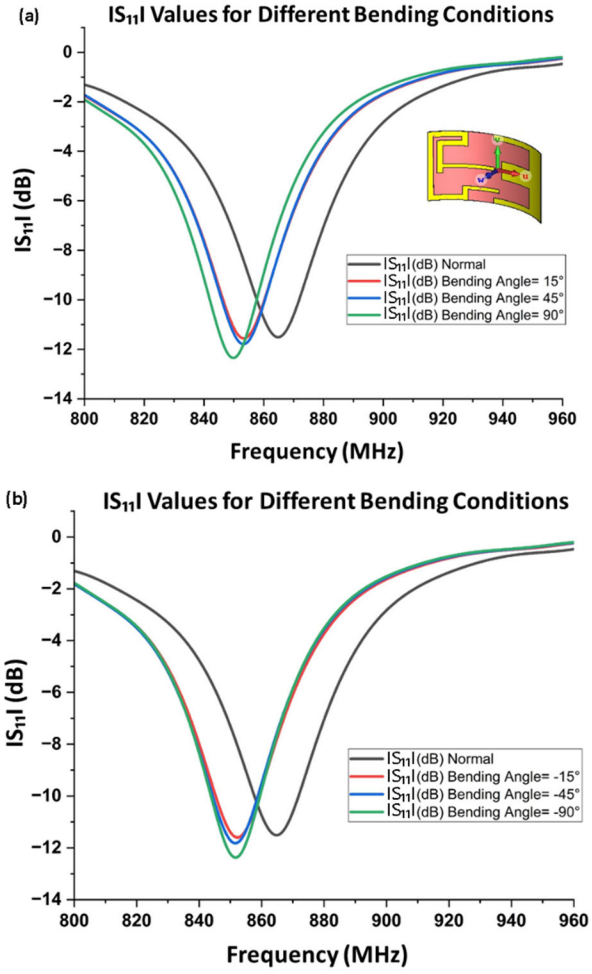

FIGURE 13. (a) |S11| values of RFID sensor structure against positive bending angles (b) |S11| values of RFID sensor structure against negative bending angles.

ranging from 15° to 90° with 15° steps have been shown in the Figure 12.

According to the Figure 12, the input impedance of RFID wetness detection sensor is severely affected due to the nearfield coupling of resonating sensor sections with the stacked human body model layers having different electric permittivity and conductivity parameters. This can be deduced from the numerically computed radiation patterns shown in Figure 3. However, the effect of different bending angles on the reflection parameter is in negligible amount.

In addition, in order to figure out the input impedance behavior of RFID sensor structure in free space without human body phantom model against different bending conditions, the reflection parameter results for different bending angles are shown in Figure 13. According to |S11| graphs given in Figure 13, when positive bending angles are applied to the structure, it is concluded that the resonance frequency of RFID sensor structure shifts to the lower frequencies with smaller than 2.3% frequency change with reference to the resonance frequency in the unbent condition. Likewise, the tendency of the structure to shift in the resonant frequency is similar when negative bending angles are applied. When the shifts in the resonance frequencies in both graphs are examined, it is seen that the shifts are quite low. Therefore, the resistance of the RFID sensor structure to bending is good.

TABLE 3. Near field RSSI measurement results of RFID sensor structure before and after deformation test.

RFID sensor situation	Average RSSI before bending (dBm)	Average RSSI after bending (dBm)	RSSI change (%)
Dry	- 35.45	- 35.48	0.09
5 mL water	- 37.60	- 37.97	0.98
9 mL water	- 38.90	- 39.23	0.86
11 mL water	- 40.28	- 40.95	1.68
15 mL water	- 42.09	- 42.56	1.12
30 mL water	- 48.98	- 49.62	1.30
45 mL water	- 53.02	- 54.92	1.69

TABLE 4. RSSI values of RFID sensor structure with diaper for different bending angles at 30 CM.

Bending angles (°)	Maximum RSSI after bending (dBm)
0	- 23.50
15	- 26.00
20	- 28.50
25	- 28.50
30	- 29.00
40	- 29.50

In addition to the numerical computations, a deformation test has been applied to the RFID sensor structure integrated onto the adult diaper. The RSSI values of the RFID sensor structure in the dry and wetted with water state before and after deformation are measured in near field measurement setup shown in Figure 7. The RSSI values measured after a total of 10 deformation cycles are shown in Table 3. According to the percent RSSI changes given in Table 3, it is seen that the difference between the RSSI values measured before and after deformation for each condition is quite small. This situation shows that the RFID sensor structure performs well even after 10 cycle deformation. The main purpose of the deformation test is to have an idea of how the stress resulting from bending the RFID sensor can affect the solders of the chip integrated onto the RFID sensor. While applying different bending angles to the chip integrated sensor, it has been determined that the soldered chip could be disconnected from the attached points at angles above 30°. Therefore, the threshold bending angle is determined to be 30°. In addition to these studies, a bending test has been applied to the RFID sensor integrated diaper in the dry state. The RSSI values measured according to the bending at different angles applied to the diaper have been indicated in the Table 4. Table 5 indicates the comparison of this study with the other studies

TABLE 5. Comparison of passive RFID diaper wetness sensors.

Wireless Technology	Sensing Principle	Fabrication Method	Dimensions	Detection	Reading Range	Polarization	Flexible	Disposable	User Testing	Ref.
Passive UHF RFID	Received signal strength indicator (RSSI)	Hand fabrication (Hydrogel-metal hybrid tags)	<100 × 80 × 20 mm³	Dry/wet	1.0 m	NA	Yes	Yes	Testing with doll	[23]
Semi-passive HF RFID	Built-in energy conversion sensor (Action-Activated Tag)	Screen printing	<5 × 5 mm² (for sensor) ~25 × 35 mm² (for tag)	Dry/wet	1.5 m	NA	NA	Yes	NA	[43]
Passive HF RFID	Near-field inductive coupling of the transponder tag	Attaching the tag antenna, metal sheet and paper	~3×3 mm²	Dry/wet	0.12 m	NA	Yes	NA	Testing with adult	[44]
Passive UHF RFID	Received signal strength indicator (RSSI)	Commerciall y available (Monza E64 Viper tag antenna)	105 × 6 × 0.1 mm³	Dry/wet	4.4 m (adult) 3.6 m (baby)	Considered	Yes	Disposable/ Reusable	Testing with human avatar	[36]
Passive HF RFID	Received signal strength indicator (RSSI)	Conductive tracks	550 × 300 mm²	Dry/wet	0.263 m	NA	NA	Yes	Testing with adult man	[45]
Passive UHF RFID	Degradation of the antenna performance	Commerciall y available (Gen-2 RFID tags)	NA	Wet	1.4 m	NA	NA	NA	Testing in laborator y	[37]
Passive UHF RFID	Received signal strength indicator (RSSI)	Pad printing	75 × 38 × 0.12 mm³	Dry/wet	NA	NA	Yes	Yes	Testing in laborator y	This work

on diaper wetness sensor. When other passive RFID wetness sensor for urinary incontinence are evaluated in the literature, polarization is considered in very few studies and it is generally linear polarization. Although it can be implied that the polarization mismatch effect can cause approximately 20 dBm signal degradation in RSSI level, the reliable reading performance can be still accomplished at maximum reading range of 50 cm in wet state.

IV. CONCLUSION

In this study, wearable and flexible RFID sensor structure that operates in UHF RFID band has been designed and then fabricated using pad printing machine. Two different types of RSSI measurements have been carried out to determine the behavior of the RFID sensor structure against wetness to point out the technical applicability potential of the proposed wetness sensor. Water, saline, and urine solutions are dropped onto the RFID sensor to simulate different wetting conditions while conducting the multiple RSSI measurements in the near field with the result of at least 17 dBm signal difference in measured RSSI values between the dry and wet states. RF performance of the proposed RFID wetness detection sensor has been investigated in more practical applications with three different separation distances ranging from 32 cm up to 50 cm. The maximum reliable reading range of the RFID sensor is determined to be 50 cm under the different polarization angles with respect to the reader antenna in wet state. According to the results obtained, the proposed RFID sensor structure can detect wetness with varying RSSI values. At the same time, the bending test has been applied to the RFID sensor integrated onto the adult diaper to evaluate the performance of the RFID sensor structure against bending. As a result, it is implied that the RSSI values of the structure after bending are changed quite little compared to the RSSI values before the bending. In addition, the dimensions of the developed sensor are very suitable for the integration onto adult diapers or pads. It is thought that the proposed sensor structure can be used to detect wetness situations such as urinary incontinence.

REFERENCES

[1] F. Costa, S. Genovesi, M. Borgese, A. Michel, F. A. Dicandia, and G. Manara, "A review of RFID sensors, the new frontier of Internet of Things," *Sensors*, vol. 21, no. 9, p. 3138, Apr. 2021, doi: 10.3390/s21093138.

[2] J. C. Prather, Y. Meng, M. Bolt, T. Horton, and M. Adams, "Wireless head impact monitoring system utilizing eye movement as a surrogate for brain movement," *AEU Int. J. Electron. Commun.*, vol. 105, pp. 54–61, Jun. 2019, doi: 10.1016/j.aeue.2019.04.003.

[3] S. Xie, C. Ma, R. Feng, X. Xiang, and P. Jiang, "Wireless glucose sensing system based on dual-tag RFID technology," *IEEE Sensors J.*, vol. 22, no. 13, pp. 13632–13639, Jul. 2022.

[4] Y. Shafiq, J. S. Gibson, H. Kim, C. P. Ambulo, T. H. Ware, and S. V. Georgakopoulos, "A reusable battery-free RFID temperature sensor," *IEEE Trans. Antennas Propag.*, vol. 67, no. 10, pp. 6612–6626, Oct. 2019, doi: 10.1109/TAP.2019.2921150.

[5] Q. Cao, D. R. Jones, and H. Sheng, "Contained nomadic information environments: Technology, organization, and environment influences on adoption of hospital RFID patient tracking," *Inf. Manage.*, vol. 51, no. 2, pp. 225–239, Mar. 2014, doi: 10.1016/j.im.2013.11.007.

[6] W. Wanhua, "Design and research of logistics distribution system based on RFID," *J. Phys., Conf. Ser.*, vol. 1544, no. 1, May 2020, Art. no. 012193, doi: 10.1088/1742-6596/1544/1/012193.

[7] M. C. Caccami, S. Amendola, and C. Occhiuzzi, "Method and system for reading RFID tags embedded into tires on conveyors," in *Proc. IEEE Int. Conf. RFID Technol. Appl. (RFID-TA)*, Sep. 2019, pp. 141–144, doi: 10.1109/RFID-TA.2019.8892245.

[8] C. Luo, I. Gil, and R. Fernández-García, "Electro-textile UHF-RFID compression sensor for health-caring applications," *IEEE Sensors J.*, vol. 22, no. 12, pp. 12332–12338, Jun. 2022, doi: 10.1109/JSEN.2022.3172506.

[9] C. Luo, I. Gil, and R. Fernández-García, "Wearable textile UHF-RFID sensors: A systematic review," *Materials*, vol. 13, no. 15, p. 3292, Jul. 2020, doi: 10.3390/ma13153292.

[10] F. Gaspari and S. Quaranta, "Nanostructured Materials for RFID sensors," in *Nanomaterials Design for Sensing Applications*. Amsterdam, The Netherlands: Elsevier, 2019.

[11] A. Vena, B. Sorli, B. Saggin, R. Garcia, and J. Podlecki, "Passive UHF RFID sensor to monitor fragile objects during transportation," in *Proc. IEEE Int. Conf. RFID Technol. Appl. (RFID-TA)*, Sep. 2019, pp. 415–420, doi: 10.1109/RFID-TA.2019.8892033.

[12] M. A. S. Tajin, C. E. Amanatides, G. Dion, and K. R. Dandekar, "Passive UHF RFID-based knitted wearable compression sensor," *IEEE Internet Things J.*, vol. 8, no. 17, pp. 13763–13773, Sep. 2021, doi: 10.1109/JIOT.2021.3068198.

[13] I. Akdag, C. Gocen, M. Palandoken, and A. Kaya, "A novel circularly polarized reader antenna design for UHF RFID applications," *Wireless Netw.*, vol. 28, no. 6, pp. 2625–2636, Aug. 2022, doi: 10.1007/s11276-022-02998-8.

[14] M. Frigerio, M. Barba, A. Cola, G. Marino, S. Volontè, T. Melocchi, D. De Vicari, and S. Maruccia, "Flat magnetic stimulation for stress urinary incontinence: A prospective comparison study," *Bioengineering*, vol. 10, no. 3, p. 295, Feb. 2023, doi: 10.3390/bioengineering10030295.

[15] A. Alizadeh, S. Mohammah-Alizadeh-Charandabi, L. Khodaie, and M. Mirghafourvand, "Effect of *Nigella sativa L.* Seed oil on urinary incontinence and quality of life in menopausal women: A triple-blind randomized controlled trial," *Phytotherapy Res.*, vol. 37, no. 5, pp. 2012–2023, May 2023, doi: 10.1002/ptr.7725.

[16] A. Alizadeh, M. Montazeri, F. Shabani, S. Bani, S. Hassanpour, M. Nabighadim, and M. Mirghafourvand, "Prevalence and severity of urinary incontinence and associated factors in Iranian postmenopausal women: A cross-sectional study," *BMC Urology*, vol. 23, no. 1, pp. 1–9, Feb. 2023, doi: 10.1186/s12894-023-01186-w.

[17] M. C. Michel, L. Cardozo, C. J. Chermansky, F. Cruz, Y. Igawa, K.-S. Lee, A. Sahai, A. J. Wein, and K.-E. Andersson, "Current and emerging pharmacological targets and treatments of urinary incontinence and related disorders," *Pharmacol. Rev.*, vol. 75, no. 4, pp. 554–674, Jul. 2023.

[18] J. Ho Cho, J.-Y. Choi, N.-H. Kim, Y. Lim, J. Hun Ohn, E. Sun Kim, J. Ryu, J. Kim, Y. Kim, S.-W. Kim, and K.-I. Kim, "A smart diaper system using Bluetooth and smartphones to automatically detect urination and volume of voiding: Prospective observational pilot study in an acute care hospital,", vol. 23, no. 7, e29979, doi: 10.2196/preprints.29979.

[19] A. K. Jaekel, T. M. Rings, F. Schmitz, F. Knappe, A. Tschirhart, F. I. Winterhagen, R. K. M. Kirschner-Hermanns, and S. C. Knüpfer, "Urinary and double incontinence in cognitively impaired patients: Impacts on those affected and their professional caregivers," *J. Clin. Med.*, vol. 12, no. 10, p. 3352, May 2023, doi: 10.3390/jcm12103352.

[20] C. Luo, I. Gil, and R. Fernández-García, "Textile UHF-RFID antenna embroidered on surgical masks for future textile sensing applications," *IEEE Trans. Antennas Propag.*, vol. 70, no. 7, pp. 5246–5253, Jul. 2022, doi: 10.1109/TAP.2022.3145477.

[21] D. Shuaib, L. Ukkonen, J. Virkki, and S. Merilampi, "The possibilities of embroidered passive UHF RFID textile tags as wearable moisture sensors," in *Proc. IEEE 5th Int. Conf. Serious Games Appl. for Health (SeGAH)*, Apr. 2017, pp. 1–5, doi: 10.1109/SeGAH.2017.7939286.

[22] M. Tekcin, S. Paker, and S. K. Bahadir, "UHF-RFID enabled wearable flexible printed sensor with antenna performance," *AEU Int. J. Electron. Commun.*, vol. 157, Dec. 2022, Art. no. 154410, doi: 10.1016/j.aeue.2022.154410.

[23] P. Sen, S. N. R. Kantareddy, R. Bhattacharyya, S. E. Sarma, and J. E. Siegel, "Low-cost diaper wetness detection using hydrogel-based RFID tags," *IEEE Sensors J.*, vol. 20, no. 6, pp. 3293–3302, Mar. 2020, doi: 10.1109/JSEN.2019.2954746.

[24] M. Y. E. Simik, F. Chi, and C. L. Wei, "Design and implementation of a Bluetooth-based MCU and GSM for wetness detection," *IEEE Access*, vol. 7, pp. 21851–21856, 2019, doi: 10.1109/ACCESS.2019.2897324.

[25] M. Fischer, M. Renzler, and T. Ussmueller, "Development of a smart bed insert for detection of incontinence and occupation in elder care," *IEEE Access*, vol. 7, pp. 118498–118508, 2019, doi: 10.1109/ACCESS.2019.2931041.

[26] M. Beltrão, F. M. Duarte, J. C. Viana, and V. Paulo, "A review on in-mold electronics technology," *Polym. Eng. Sci.*, vol. 62, no. 4, pp. 967–990, Apr. 2022, doi: 10.1002/pen.25918.

[27] M. Tekcin, B. A. Kuzubasoglu, E. Sayar, M. K. Yalcin, and S. K. Bahadir, "Performance analysis of wearable and flexible humidity sensor integrated to face mask for respiration monitoring," in *Proc. IEEE 3rd Eurasia Conf. IOT, Commun. Eng. (ECICE)*, Oct. 2021, pp. 663–666.

[28] M. Tekcin, E. Sayar, M. K. Yalcin, and S. K. Bahadir, "Wearable and flexible humidity sensor integrated to disposable diapers for wetness monitoring and urinary incontinence," *Electronics*, vol. 11, no. 7, p. 1025, Mar. 2022, doi: 10.3390/electronics11071025.

[29] C. Cooper and B. Hughes, "Aerosol jet printing of electronics: An enabling technology for wearable devices," in *Proc. Pan Pacific Microelectron. Symp. (Pan Pacific)*, Feb. 2020, pp. 1–11, doi: 10.23919/PanPacific48324.2020.9059444.

[30] X. Qi, H. Ha, B. Hwang, and S. Lim, "Printability of the screen-printed strain sensor with carbon Black/Silver paste for sensitive wearable electronics," *Appl. Sci.*, vol. 10, no. 19, p. 6983, Oct. 2020, doi: 10.3390/app10196983.

[31] M. Bariya, Z. Shahpar, H. Park, J. Sun, Y. Jung, W. Gao, H. Y. Y. Nyein, T. S. Liaw, L.-C. Tai, Q. P. Ngo, M. Chao, Y. Zhao, M. Hettick, G. Cho, and A. Javey, "Roll-to-roll gravure printed electrochemical sensors for wearable and medical devices," *ACS Nano*, vol. 12, no. 7, pp. 6978–6987, Jul. 2018, doi: 10.1021/acsnano.8b02505.

[32] Y. Wang, Y. Huang, Y.-Z. Li, P. Cheng, S.-Y. Cheng, Q. Liang, Z.-Q. Xu, H.-J. Chen, and Z.-S. Feng, "A facile process combined with roll-to-roll flexographic printing and electroless deposition to fabricate RFID tag antenna on paper substrates," *Composites Part B: Eng.*, vol. 224, Nov. 2021, Art. no. 109194, doi: 10.1016/j.compositesb.2021.109194.

[33] A. Jaafar, S. Schoinas, and P. Passeraub, "Pad-printing as a fabrication process for flexible and compact multilayer circuits," *Sensors*, vol. 21, no. 20, p. 6802, Oct. 2021, doi: 10.3390/s21206802.

[34] Y. Xiong and Z. Qu, "Antenna 3D pad printing solution evaluation," in *Proc. IEEE Int. Symp. Antennas Propag. (APSURSI)*, Jul. 2011, pp. 2773–2776, doi: 10.1109/APS.2011.5997101.

[35] S. L. Merilampi, T. Björninen, L. Ukkonen, P. Ruuskanen, and L. Sydänheimo, "Characterization of UHF RFID tags fabricated directly on convex surfaces by pad printing," *Int. J. Adv. Manuf. Technol.*, vol. 53, nos. 5–8, pp. 577–591, Mar. 2011, doi: 10.1007/s00170-010-2869-y.

[36] M. A. S. Tajin, W. M. Mongan, and K. R. Dandekar, "Passive RFID-based diaper moisture sensor," *IEEE Sensors J.*, vol. 21, no. 2, pp. 1665–1674, Jan. 2021, doi: 10.1109/JSEN.2020.3021395.

[37] H.-E. Nilsson, J. Sidén, and M. Gulliksson, "An incontinence alarm solution utilizing RFID based sensor technology," in *Proc. IEEE Int. Conf. RFID-Technol. Appl.*, Sep. 2011, pp. 359–363, doi: 10.1109/RFID-TA.2011.6068662.

[38] L. Xu, X. Chen, S. Tan, Z. Hu, B. Ying, T. T. Ye, and Y. Li, "Characterization and modeling of embroidered NFC coil antennas for wearable applications," *IEEE Sensors J.*, vol. 20, no. 23, pp. 14501–14513, Dec. 2020, doi: 10.1109/JSEN.2020.3008594.

[39] H.-K. Nie, X.-W. Xuan, Q. Shi, A. Guo, M.-J. Li, H.-J. Li, and G.-J. Ren, "Wearable antenna sensor based on EBG structure for cervical curvature monitoring," *IEEE Sensors J.*, vol. 22, no. 1, pp. 315–323, Jan. 2022, doi: 10.1109/JSEN.2021.3130252.

[40] E. A. Ozek, S. Tanyeli, and M. K. Yapici, "Flexible graphene textile temperature sensing RFID coils based on spray printing," *IEEE Sensors J.*, vol. 21, no. 23, pp. 26382–26388, Dec. 2021, doi: 10.1109/JSEN.2021.3075902.
[41] R. Colella, S. Sabina, P. Mincarone, and L. Catarinucci, "Semi-passive RFID electronic devices with on-chip sensor fusion capabilities for motion capture and biomechanical analysis," *IEEE Sensors J.*, vol. 23, no. 11, pp. 11672–11681, Jun. 2023, doi: 10.1109/JSEN.2023.3267540.
[42] Dielectric Properties of Body Tissues. (2023). [Online]. Available: http://niremf.ifac.cnr.it/tissprop/htmlclie/htmlclie.php
[43] J. Sidén, A. Koptioug, and M. Gulliksson, "The 'smart' diaper moisture detection system," in *IEEE MTT-S Int. Microw. Symp. Dig.*, vol. 2, Jun. 2004, pp. 659–662, doi: 10.1109/mwsym.2004.1336073.
[44] M. A. Ziai and J. C. Batchelor, "Smart radio-frequency identification tag for diaper moisture detection," *Healthcare Technol. Lett.*, vol. 2, no. 1, pp. 18–21, Feb. 2015, doi: 10.1049/htl.2014.0098.
[45] K. Yamada, N. Toshiaki, K. Ishihara, Y. Ohno, A. Ishii, S. Shimizu, T. Araki, R. Takahashi, H. Takahashi, and E. Shimizu, "Development of new type incontinence sensor using RFID tag," in *Proc. IEEE Int. Conf. Syst., Man Cybern.*, Oct. 2010, pp. 2695–2700, doi: 10.1109/ICSMC.2010.5641889.

MELTEM TEKCIN received the B.Sc. and M.S. degrees in textile engineering from İstanbul Technical University (ITU), Turkey, in 2014 and 2016, respectively, where she is currently pursuing the Ph.D. degree with the Department of Textile Engineering. She is also a Research Assistant with the Faculty of Textile Technologies and Design, ITU. Her research interests include wearable electronics, textile-based sensors and antennas, and conductive particles.

MERIH PALANDOKEN (Senior Member, IEEE) received the M.Sc. degree from the Technical University of Hamburg, Germany, in 2005, and the Ph.D. degree from the Technical University of Berlin, Germany, in 2012. He is currently an Associate Professor with the Electrical and Electronics Engineering Department, İzmir Katip Celebi University. His research interests include theoretical/computational electromagnetic field in the scope of metamaterial-based active/passive microwave component design, high frequency techniques with emphasis on bioimplantable electrically small antenna design, RFID dedicated dielectric resonator reader antenna design, energy harvesting system design and machine learning assisted smart microwave systems, including high frequency electronically controllable RF ablation probe design and smart microwave component design.

SENEM KURSUN received the M.Sc. degree in industrial engineering and the joint Ph.D. degree in computer engineering from the University of Lille, France, and in textile engineering from İstanbul Technical University (ITU) with a focus on development, application, and testing of wearable electronic systems. She is currently an Associate Professor with the Faculty of Mechanical Engineering, ITU. She is an expert in wearable electronics, sensors and control systems, system modeling and optimization, intelligent systems designs, smart textiles and clothing technologies, machine learning, and deep learning (ANN and fuzzy logic). She has authored and coauthored over 80 scientific publications in international and national peer-reviewed journals and conferences. She has been involved in many projects (European or national funding) as a researcher and a coordinator in the field of intelligent systems and textile technologies. She was also awarded two international awards and one national award for textile innovation in the field of smart textiles.